Chapter 5

Sequentially Timed All-Optical Mapping Photography for Real-Time Monitoring of Laser Ablation: Breakdown and Filamentation in Picosecond and Femtosecond Regimes

Keiichi Nakagawa, Takakazu Suzuki and Fumihiko Kannari

Additional information is available at the end of the chapter

http://dx.doi.org/10.5772/intechopen.71524

Abstract

To investigate ultrafast phenomena, a novel, ultrafast imaging technique was developed. Sequentially timed all-optical mapping photography (STAMP) performs single-shot image acquisition without the need for repetitive measurements and without sacrificing high-temporal resolution and image quality. The principle of this imaging method is based on the all-optical approach, and therefore it overcomes the temporal resolution in conventional high-speed cameras. Also, STAMP's single-shot movie-shooting capability allows us to obtain sequential images of non-repetitive ultrafast dynamic phenomena. Here, we present the motion pictures of early stage dynamics during femtosecond laser ablation captured by two types of STAMP setup. Breakdown was induced by intense femtosecond laser pulse and monitored with a frame interval of 15.3 ps and a total of six frames. The movie clearly shows the plasma generation and expansion on glass surface. Also, filamentation was generated inside a glass and observed with a frame interval of 230 fs and total of 25 frames. These phenomena have previously only been observed by pump-probe imaging. STAMP is a powerful tool to understand precise processes of complex dynamics in ultrashort laser ablation.

Keywords: laser ablation, ultrafast imaging, STAMP, laser breakdown, filamentation

1. Introduction

The dynamics of laser ablation is important for laser machining [1] and laser surgery [2]. In particular, research on a femtosecond laser ablation has been performed to utilize its advantages:

high-energy efficiency, low thermal effects, precise structuring due to the multiphoton absorption process, etc. Recent studies investigate more complex mechanism in laser ablation induced by multiple burst pulses [3], optical vortex [4], and so on. For understanding these dynamics, a method for direct observation of ultrafast phenomena has been required.

In this chapter, we introduce an ultrafast photographic technique, called "sequentially timed all-optical mapping photography (STAMP)" [5] for sub-nanosecond single-shot imaging and then present motion pictures of ultrafast dynamic events in ultrashort laser ablation.

2. High-speed imaging techniques for monitoring fast process of ultrashort laser ablation

High-speed imaging is powerful tool for discovering and studying dynamic phenomena [6, 7]. Many techniques and instruments have been developed to satisfy a great demand for observation of fast events. We need to choose an appropriate method according to the phenomena what we observe. **Figure 1** shows the timescale of physical events in ultrashort laser ablation of transparent materials [8]. The dynamics of femtosecond laser ablation is characterized differently on various time scales. First, laser ablation occurs by the material's absorption of photons at t = 1 to ~100 fs. At t = ~100 fs to ~10 ps, the energy of the electrons is transferred to the lattice via carrier-phonon scattering. At t = ~10 ps to ~10 ns, a shockwave and plume are formed at and propagate from the focal volume. Also, on the same time scale, the thermal

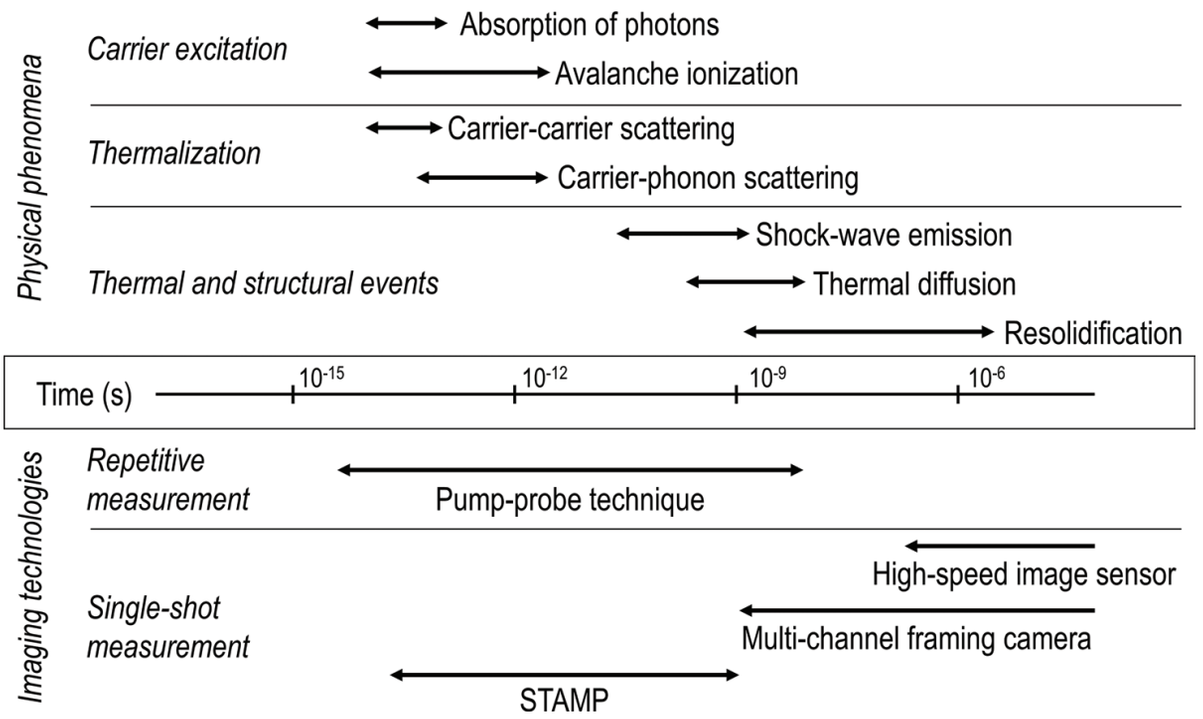

Figure 1. Timescale of physical events in ultrashort laser ablation and high-speed imaging technologies. The upper part of this figure is illustrated based on [8].

energy diffuses from the focal volume. In the bottom half of **Figure 1**, the characteristic of imaging technologies is summarized. Here, we review pump-probe technique and conventional high-speed cameras and introduce STAMP.

2.1. Conventional techniques for capturing ablation dynamics

Time-resolved imaging based on the pump-probe technique is a popular method for studying ultrafast dynamic events in laser ablation. Its principle is the construction of a time-resolved motion picture from repetitive measurements with different time delays between the trigger pulse (pump) and measurement pulse (probe). Although the pump-probe imaging allows us to capture ultrafast phenomena with the high-temporal resolution without the need for a fast detector, it requires that the event under observation to be relatively simple and easily reproducible. It falls short in studying non-repetitive or difficult-to-reproduce events such as those found in laser ablation of biological materials and carbon fiber reinforced plastic and multi-pulse laser ablation [3].

In many fields of basic science or applied technology, the versatile video camera based on charged-coupled device (CCD) or complementary metal-oxide-semiconductor (CMOS) technology has been widely used for study of dynamic phenomena. For achieving high temporal resolution in imaging, specialized instruments (for example, the *in-situ* storage image sensor [9], rotating mirror camera [10], and multi-channel framing camera [11]) have been developed. The time response of these instruments is ~1 ns, limited due to technical limitations in mechanical and electrical components of the camera such as mechanical scanning, data readout, and shutters.

A streak camera [12] is also used for monitoring ultrafast events with a sub-nanosecond resolution. The streak camera which operates by electronically sweeping the spatial profile of the target onto an image sensor can run faster than the 2D high-speed cameras. Although the streak camera can provide a femtosecond temporal resolution, its operation is limited to 1D imaging.

2.2. Sequentially timed all-optical mapping photography for sub-nanosecond single-shot imaging

STAMP was developed in order to overcome the limitations in conventional high-speed imaging technologies and to observe non-repetitive ultrafast phenomena. It performs continuous, single-shot, burst image acquisition without the need for repetitive measurements, yet with equally high-temporal resolution and image quality.

In ultrafast events, the information we need is compressed in the time domain. When we acquire a movie in the time domain, we have to use a device or material that has a very fast response speed to resolve and take the compressed information. All of these direct approaches must face to limitations in the response speed of the device or material. In order to avoid these limitations, STAMP performs "mapping" of the target's time-varying spatial profile onto a burst stream of photographs with spatiotemporal dispersion (**Figure 2**). The camera's all-optical operation eliminates the speed bottleneck that exists in conventional burst cameras and hence enables ultrafast, multi-dimensional motion picture photography.

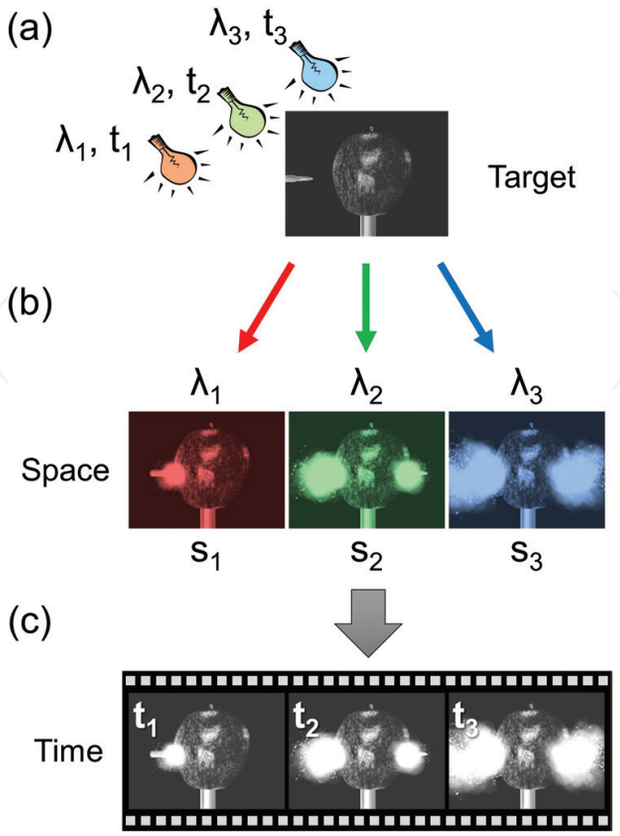

Figure 2. Principle of STAMP. (a) The target is illuminated by light with wavelength of λ_1, λ_2, and λ_3 at time t_1, t_2, and t_3. (b) The light modulated by the target is spectrally separated and detected on different positions s_1, s_2, and s_3. (c) Based on both the correspondence relation between time t and wavelength λ and the correspondence between wavelength λ and space s, the images are reconstructed as a movie.

Basic configuration of STAMP is schematically shown in **Figure 3**. It consists of an ultrashort pulse source, a temporal mapping device, a spatial mapping device, an image sensor, and a computer. The key components for realizing STAMP are a temporal mapping device and a spatial mapping device. The operation of STAMP is as follows. First, an ultrashort laser pulse generated by the laser source is temporally and spectrally shaped into a series of discrete daughter pulses by the temporal mapping device. Here, the daughter pulses correspond to different spectral bands of the original pulse. The daughter pulses are incident onto the target as successive "flashes" for stroboscopic image acquisition (which can be conducted in either the reflection or transmission mode, depending on the reflectivity profile of the target). The image-encoded daughter pulses are "passively" and "optically" separated by the spatial mapping device and incident onto different areas of the image sensor. Even though the events are very fast, we can use highly sensitive image sensors that permit microscopic imaging with low-intensity illumination. The data recorded on the image sensor are digitally processed on the computer to reconstruct motion pictures with the frame interval and exposure time calibrated from the settings of the pulse stretcher and pulse shaper in the temporal mapping device. It can be tuned, depending on the time scale of the dynamical event of interest [13]. The total number of frames can also be changed, depending on the bandwidth of the original laser pulse and the settings of the temporal and spatial mapping

http://dx.doi.org/10.5772/intechopen.71524

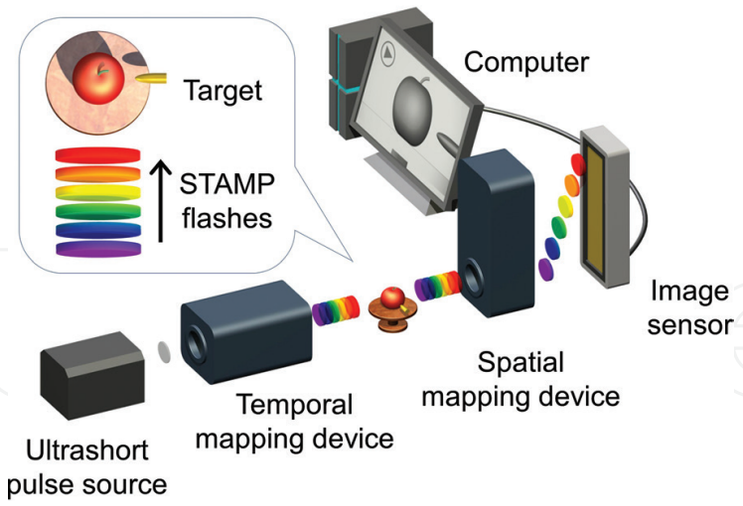

Figure 3. Basic configuration of STAMP.

devices. The speed barriers of mechanical and electrical operation can be eliminated completely, since only light emitted from the pulse source travels to the image sensor through the passive optical system.

As described above, the main feature of STAMP is its capability of sub-nanosecond multidimensional image acquisition with high image quality and without repetitive measurements. Additionally, in the STAMP operation, various imaging techniques such as interferometry, polarization imaging, and shadowgraph imaging can be employed for visualizing phenomena. On the other hand, there are some limitations in STAMP. We have to consider the potential negative effects of samples on STAMP's operation. STAMP has difficulty in being applied to photograph luminous objects. Also, we assume that the sample does not have any strong dependence on wavelength in STAMP's spectral range. In order to capture target phenomena, we need to understand these features and design its optical setup properly.

3. Real-time observation of early stage plasma evolution during femtosecond laser ablation

Here, we present movies of early stage plasma evolution during femtosecond laser ablation captured by STAMP. We focused on the picosecond timescale, where the physical dynamics in laser ablation of a transparent material transits from carrier excitation and thermalization to structural events (see **Figure 1**).

3.1. Experimental setup of ultrashort laser ablation and STAMP with spectral shaper

As shown in **Figure 4**, the surface of a glass plate was ablated by a focused femtosecond laser pulse and its resultant dynamics was observed with STAMP in transmission mode with a time resolution of a picosecond order. The ablation conditions and the detailed setup of imaging system are described below.

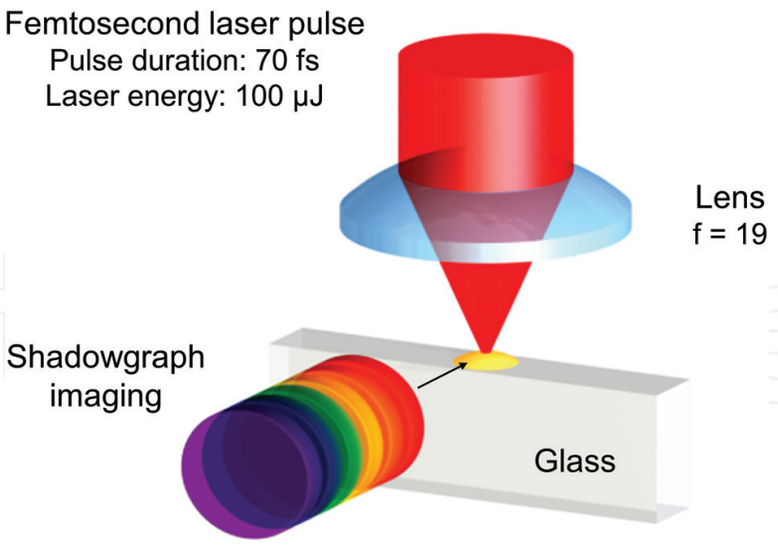

Figure 4. Experimental setup for performing and visualizing a breakdown on a glass surface in femtosecond laser ablation.

For an ultrafast laser source, we used Ti:Sapphire laser with a chirped pulse amplifier (CPA) system. The center wavelength, pulse duration, and repetition rate were 810 nm, 70 fs, and 1 kHz, respectively. The repetition rate was decreased with optical chopper as the rate of 36 Hz, and then a single pulse was generated by a mechanical shutter. This pulse was split into an excitation pulse of laser ablation and a STAMP pulse for capturing sequential images. The time difference between these two pulses was adjusted with an optical delay line. The excitation pulse with the energy of 100 μJ was focused by a lens (f = 19 mm) on the side surface of the ultrathin glass (t = 50 μm) placed in air. The power density of the laser pulse was approximately 3×10^{15} W/cm^2 at the focal point.

We developed a STAMP system that enables ultrafast motion picture photography with six frames. The developed system was composed of a femtosecond laser source which is also used for ablating materials, temporal mapping device consisting of a pulse stretcher and pulse shaper, spatial mapping device which performs spectral imaging, cooled CCD camera, and computer (**Figure 5**). In the pulse stretcher, the picosecond chirped pulse was produced from a femtosecond pulse through a grating pair for monitoring dynamic events in picosecond regime. The pulse shaper, based on the 4*f* optical configuration [14], was used as an amplitude modulator to tailor the intensity of each daughter pulse. For visualizing laser ablation dynamics, shadowgraph technique was employed. The STAMP's daughter pulses coming from the temporal mapping device illuminated the ablation area. The phenomena were imaged with an objective (10×, NA = 0.25). Here, the effects of chromatic aberration and wavelength dependence can be negligible because the difference of wavelength in each daughter pulse is around 3 nm. And then, the daughter pulses are separated by a spectral shaper [15]. The spectral shaper we developed is one of the snapshot multispectral imaging methods which perform image separation with passive optical elements [16]. In the spectral shaper, a periscope array is placed at the Fourier plane in the 4*f* configuration of the spectral shaper (**Figure 6**). The daughter pulses are diffracted by the first diffraction optics and then are focused onto the

http://dx.doi.org/10.5772/intechopen.71524

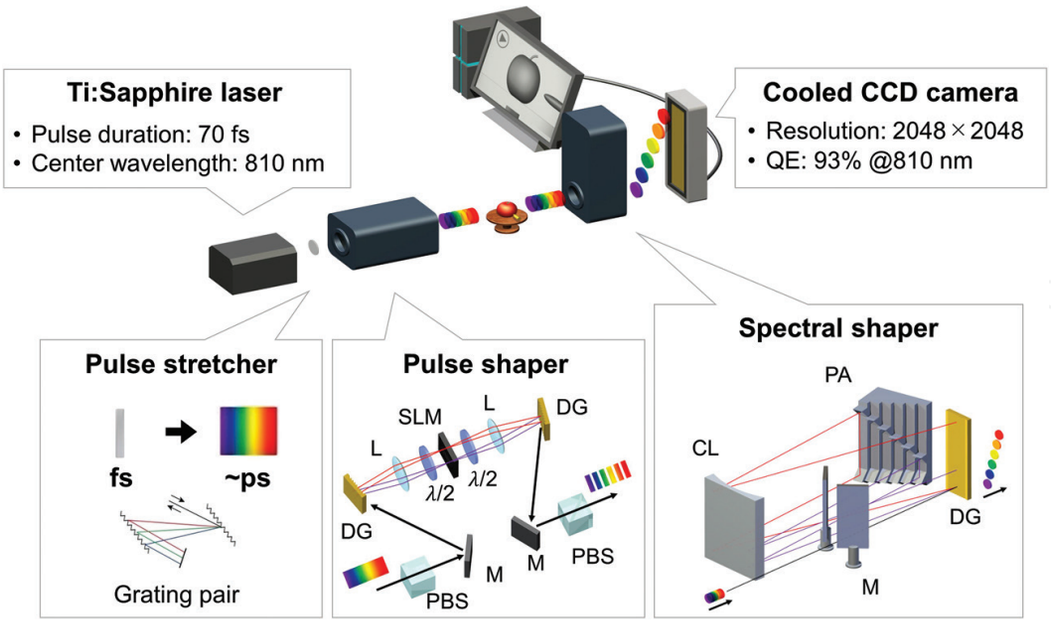

Figure 5. The schematic of STAMP utilizing the spectral shaper. CL: cylindrical lens, DG: diffraction grating, L: lens, M: mirror, PA: periscope array, PBS: polarizing beam splitter, SLM: spatial light modulator, $\lambda/2$: half wave plate.

periscope array. Each different spectral component reflects back, but comes out at a different height. Then, the daughter pulses are recombined at the second diffraction grating, but exit at different heights, keeping the spatial profile in each spectral component intact. Here, we used the periscope array having six periscopes. These daughter pulses were detected on the different position of the high-sensitive image sensor (2048 × 2048 pixels). Finally, detected images were arranged in order corresponding to the arrival time at the target.

The time difference of arrival (corresponding to the frame interval) and pulse duration (corresponding to the exposure time) of each daughter pulse was measured by the technique of cross correlation based on sum frequency generation. The optical setup is shown in **Figure 7**.

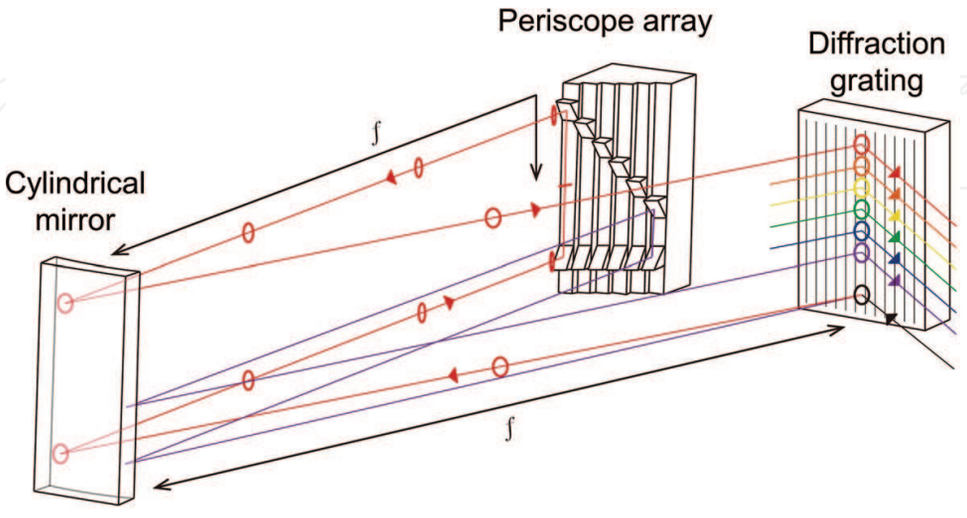

Figure 6. Configuration of the spectral shaper.

Here, each daughter pulse was produced by the pulse shaper and characterized one by one. **Figure 8** shows the temporal profile. The averaged frame interval and exposure time in this STAMP setup were 15.3 and 13.8 ps, respectively.

Figure 9 shows the microscopic images of a micrometer. The field of view and pixel resolution were 148 × 122 μm^2 and 680 × 560 pixels, respectively.

3.2. Plasma generation and expansion around glass surface

Figure 10 shows STAMP's motion picture of the generation and expansion of plume. Frames 1–3 indicate the generation of a flat plume, whereas frames 4–6 indicate its propagation in the upper direction. In frames 2–6, the process of carrier-phonon scattering is indicated by the

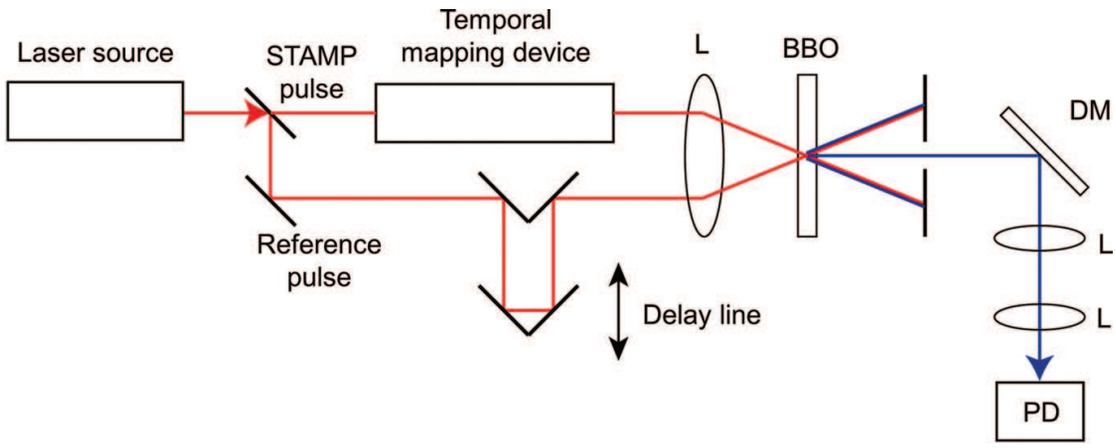

Figure 7. Schematic of the optical setup for characterizing the STAMP pulses. DM: dichroic mirror, L: lens, PD: photodiode.

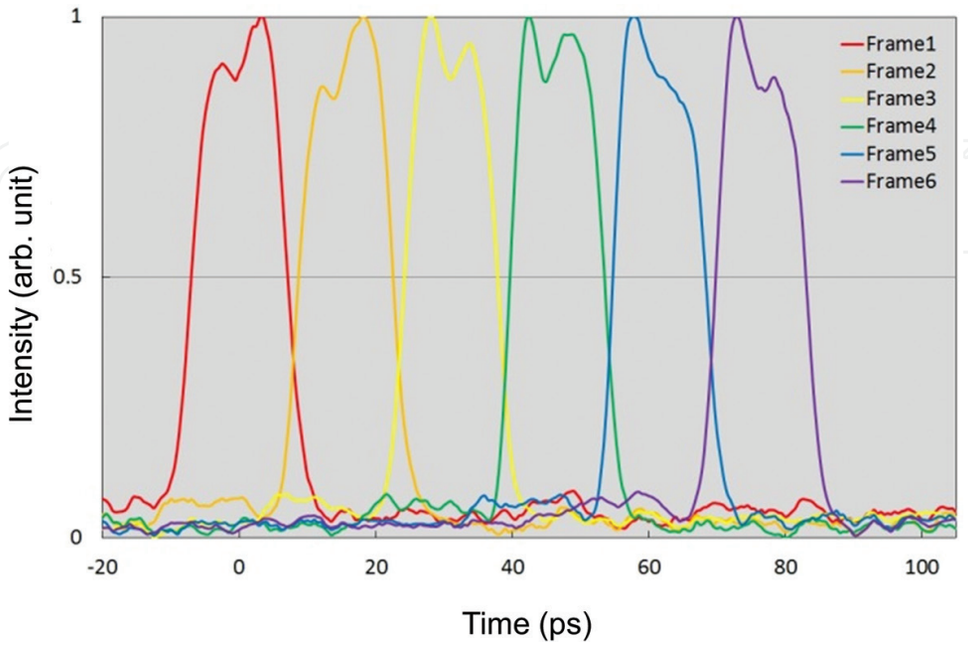

Figure 8. Temporal profile of STAMP pulses. An average frame interval and an exposure time are 15.3 and 13.8 ps, respectively [5].

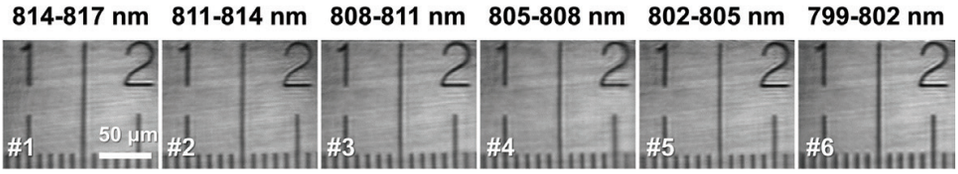

Figure 9. Image of test target. The images were captured and processed with the resolution of 680 × 560 pixels. The scale bar shows 50 μm [5].

dark region (white arrow in **Figure 10**) that corresponds to the high density of electrons in the plasma state caused by the material's absorption of light. This observation agrees well with previous reports [17].

The detailed analysis shows a slight asymmetry in the plume's wavefront profile (**Figure 11**). This is due to the fact that the ablation pulse's angle of incidence was not exactly perpendicular to the air-glass interface. The error bars in **Figure 11** are due to the ambiguity in image contrast. From the movie, the propagation speed of the plume's wavefront is found to be ~100 km/s (90°), which agrees with previously reported values [18, 19].

Figures 12 and **13** are the motion pictures of the dynamic events in femtosecond laser ablation. Although the experiment parameters such as laser intensity, beam profile, and material were not changed, the difference in evolution of a plasma plume was observed. A fluctuation

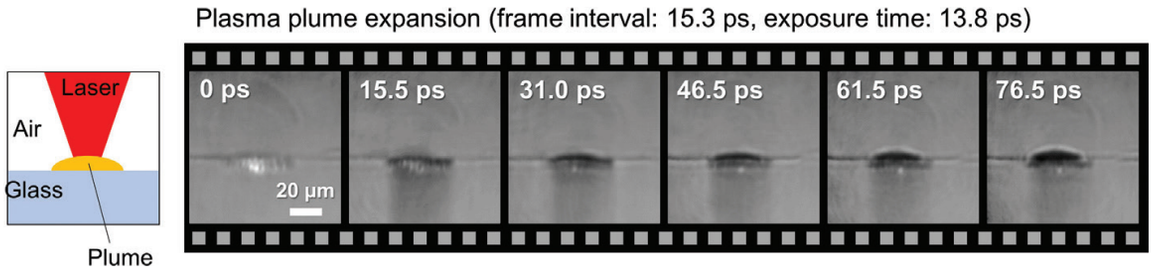

Figure 10. Motion picture of plasma generation and expansion in femtosecond laser ablation [5].

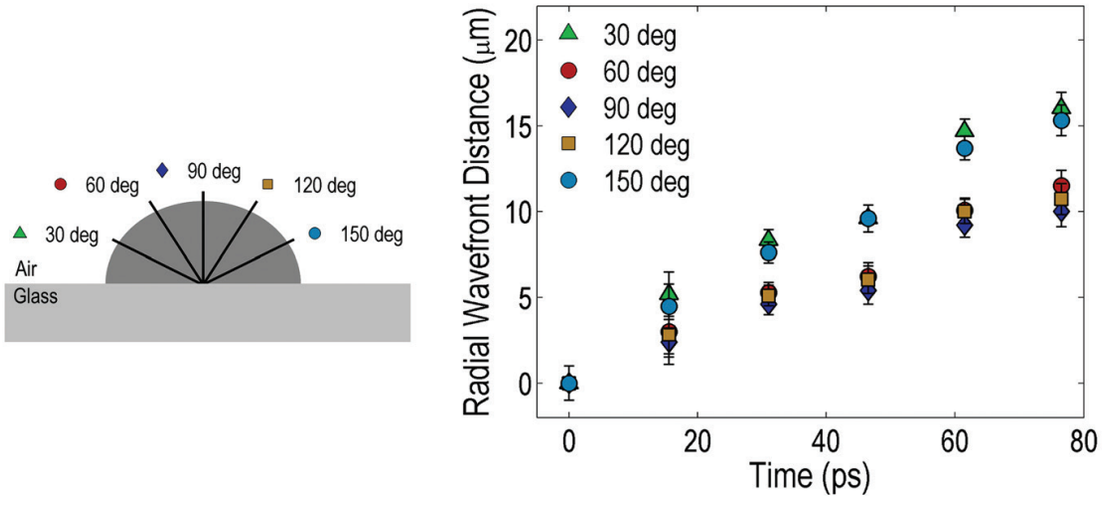

Figure 11. Analysis of evolution of the plume wavefront [5].

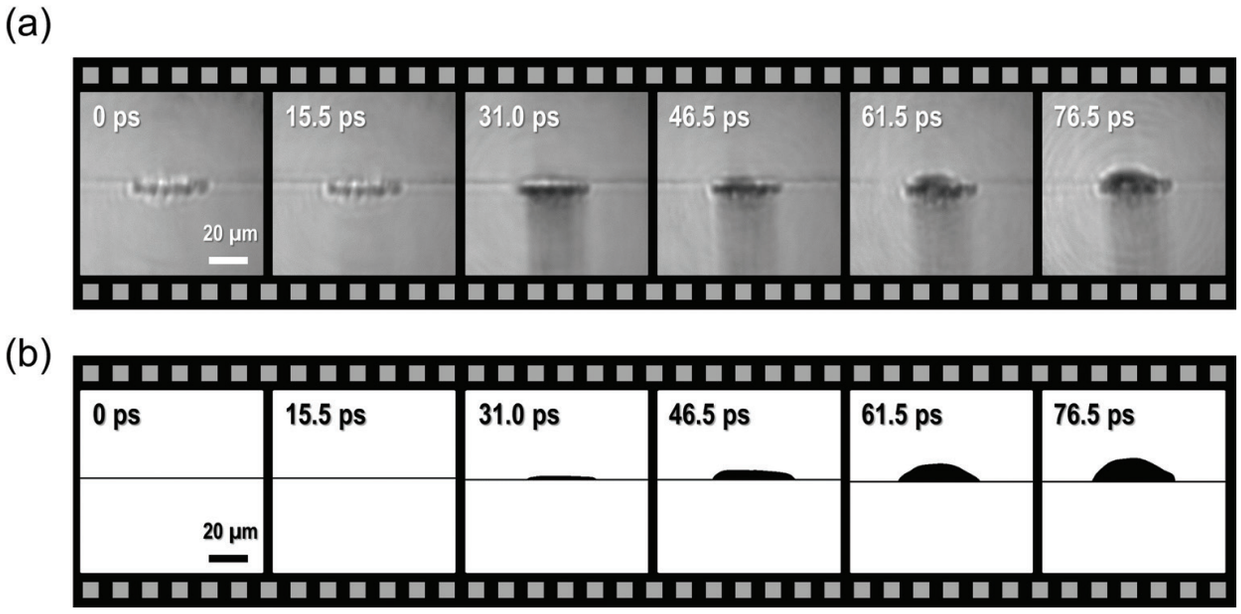

Figure 12. Motion picture of laser ablation (a) and its binarized image (b).

of the laser pulse and non-uniformity of the surface roughness of the glass often decrease the reproducible of laser ablation. STAMP is an effective tool to study a series of transitions in such difficult-to-reproduce phenomena.

We also observed shockwave emission caused as a subsequent event of plasma generation. The shock front is clearly visualized in each frame. The shock speed is quite slow comparing to the frame interval of this experimental setup and hence the difference between each image is not large (**Figure 14**).

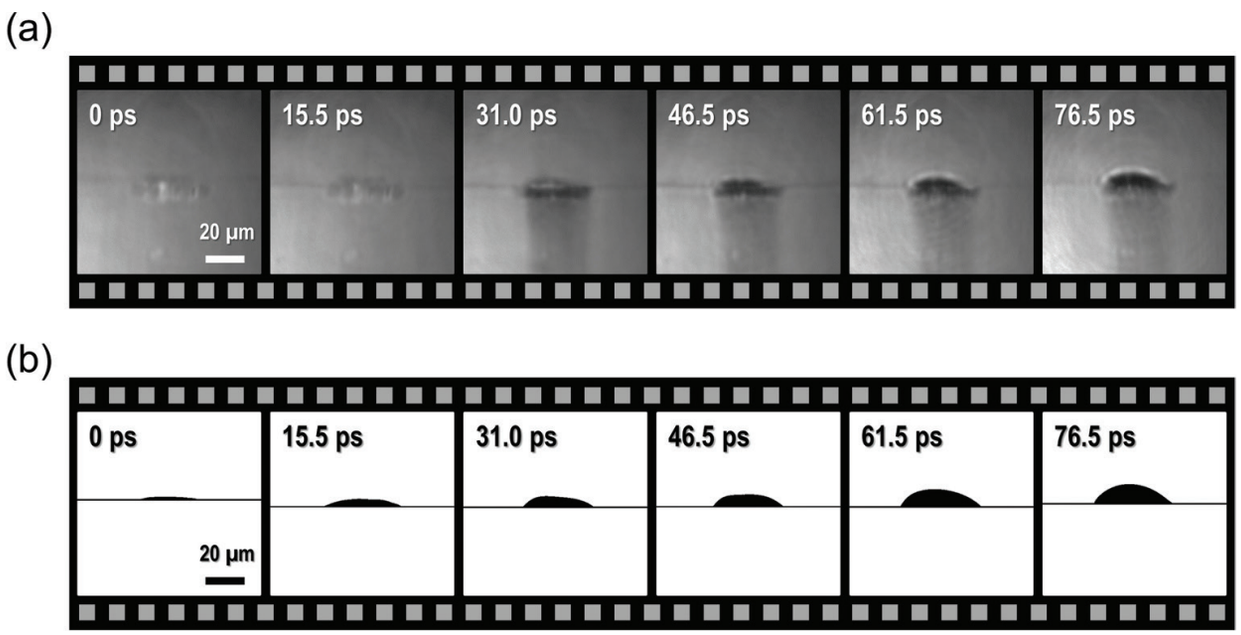

Figure 13. Motion picture (a) and binarized image (b) of laser ablation induced under the same conditions as those in the experiment of **Figure 12**.

http://dx.doi.org/10.5772/intechopen.71524

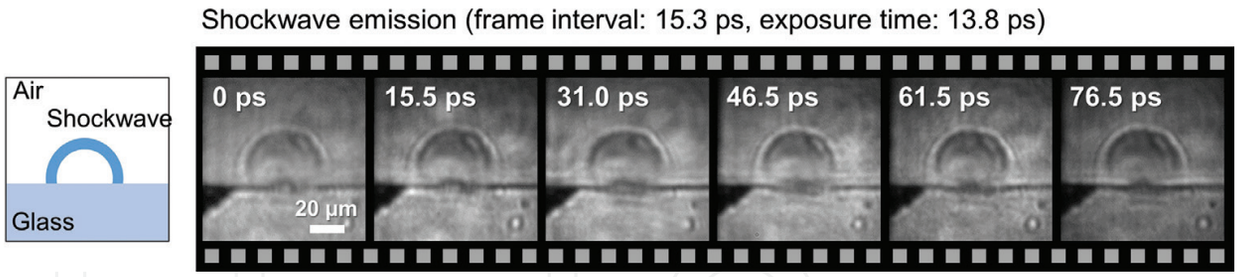

Figure 14. Motion picture of shockwave emission after breakdown.

4. Real-time monitoring of plasma filament generated by femtosecond laser inside a glass

In STAMP, the temporal resolution can be increased to the femtosecond timescale by tuning the pulse stretcher. For observing a detailed process in filamentation induced by intense femtosecond laser, the number of frame was also increased. Here, we present movies of plasma filament generated inside a glass acquired by an improved STAMP system, called SF-STAMP (STAMP utilizing spectral filtering) [20–22].

4.1. Experimental setup of filamentation and STAMP with spectral filtering

Figure 15 shows the schematic of experimental setup. A single pulse was produced from the Ti: Sapphire laser system as the same way described in Section 3.1. The center wavelength, pulse duration, and energy of excitation pulse were 800 nm, 50 fs, and 30 μJ, respectively. The femtosecond pulse was split into a STAMP pulse and an excitation pulse, and the excitation pulse was focused inside the glass with a lens (f = 8 mm).

For capturing the filamentation with 25 frames and higher temporal resolution, we improved our STAMP system by utilizing spectral broadening with an Ar-gas filled hollow core fiber and spectral filtering with a combination of a diffractive optical element (DOE) and band-pass filter (BPF). As shown in **Figure 16**, the STAMP pulse was focused into the Ar-gas filled hollow

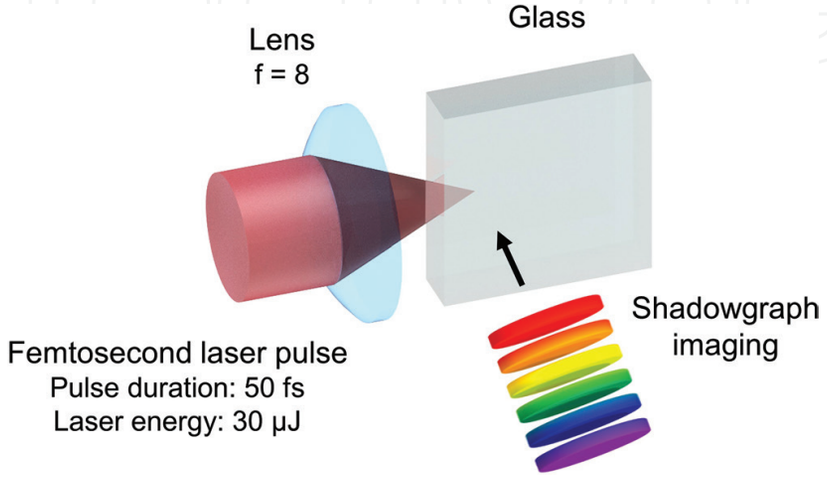

Figure 15. Experimental setup for monitoring filamentation generated by femtosecond laser.

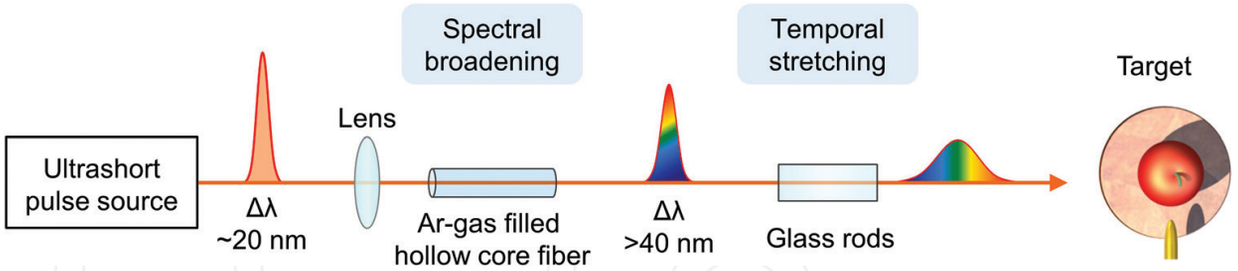

Figure 16. Temporal mapping device with an Ar-gas filled hollow core fiber for spectral broadening and with glass rods for recording with high temporal resolution.

core fiber (the length and core diameter are 400 mm and 126 μm, respectively) to produce a broadband pulse in the process of self-phase modulation. We used spectral components from 785 to 825 nm (bandwidth of 40 nm) in the broadband pulse which had nearly the uniform intensity in this spectral range. For monitoring the filamentation with higher temporal resolution, the pulse was stretched with glass rods. With the dispersion parameter and length of the glass roads, the time window and frame interval are calculated to be 5.6 ps and 230 fs, respectively. STAMP utilizing spectral filtering (SF-STAMP) has another type of the spatial mapping device which is based on the scheme of "spatially and temporally resolved intensity and phase evaluation device: full information from a single hologram (STRIPED FISH)" [23, 24]. The optical setup of the spatial mapping device in SF-STAMP was composed of a DOE, a BPF (a center wavelength of 830 nm and a bandwidth of 2.2 nm), and two lenses ($f_1 = f_2 = 50$ mm) arranged in the 4*f* configuration as shown in **Figure 17**. Since the bandwidth of the STAMP pulse was sufficiently broadened, the number of frames in this STAMP setup was determined to be 25 frames by the diffraction property of the DOE which produces 25 array beams from a single beam. While the target profile was transferred on an image sensor by the two lenses, the image-encoded chirped pulse was split into 25 pulses by the DOE place at the Fourier plane. And then these diffracted pulses were resolved by the tilted BPF depending on their

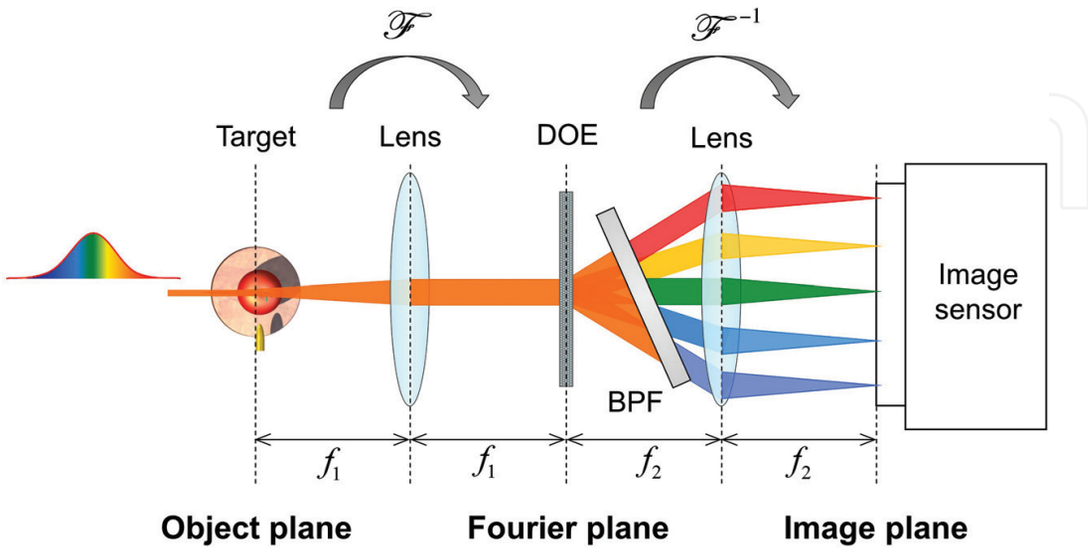

Figure 17. Spectral filtering. BPF: band-pass filter, DOE: diffractive optical element.

http://dx.doi.org/10.5772/intechopen.71524

incident angles without losing the image information. As a result, the time-varying target profiles were mapped on the different position of the image sensor. Although the much energy of an illumination pulse is needed at the target in SF-STAMP comparing to STAMP utilizing the spectral shaper, the spatial mapping device of SF-STAMP becomes compact and easy to use.

The dynamic phenomena were visualized with shadowgraph technique. **Figure 18** shows the image(s) of a resolution test chart detected by the SF-STAMP with a cooled CCD camera (4872 × 3248 pixels). The image of the left end is frame 1 of a motion picture, and the image of the right end is frame 25 projected by the spectral component which arrived at the target 5.6 ps after the arrival of the first spectral component. These frames were clipped as movie frames with the pixel resolution of 740 ×480 pixels.

4.2. Femto-to-picosecond dynamics of plasma filaments inside a glass

Figure 19 is the 25-frame movie showing the change of the refractive index inside the glass induced by the focusing of femtosecond laser. In frame 5, a dielectric breakdown appears at the center of the image. In frames 7–9, the change of intensity gradually increases. From frame 11, this dark region grows to the shape of a filament. In frame 25, the dark spot that corresponds to the high electron density in plasma state and also filamentation around the spot are clearly observed. This phenomenon occurring in the femtosecond-to-picosecond timescale has previously only been observed by pump-probe imaging in which a sample is replaced in every measurement. This demonstration highlights the utility of STAMP's single-shot movie-shooting capability.

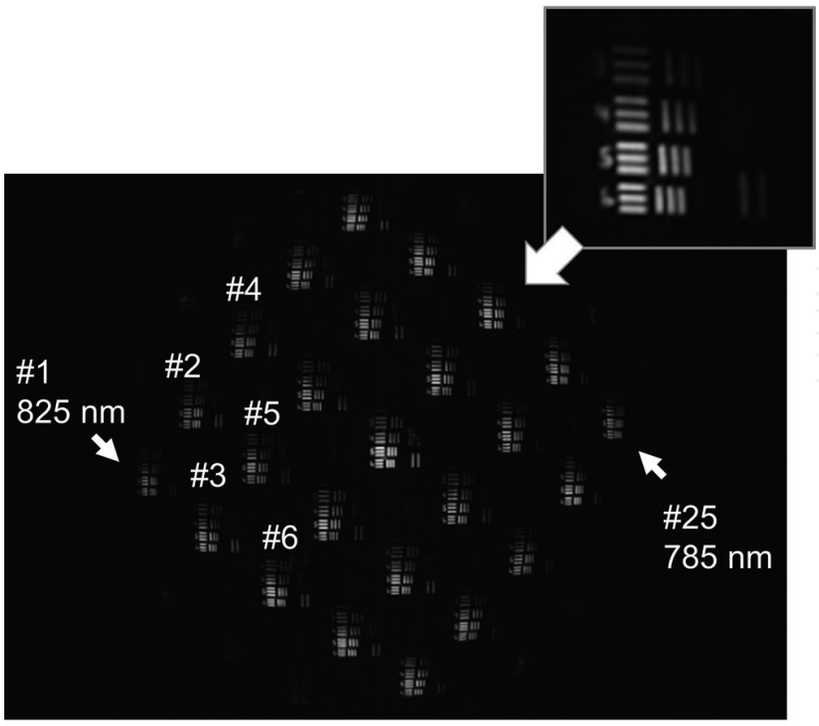

Figure 18. Image of a resolution chart.

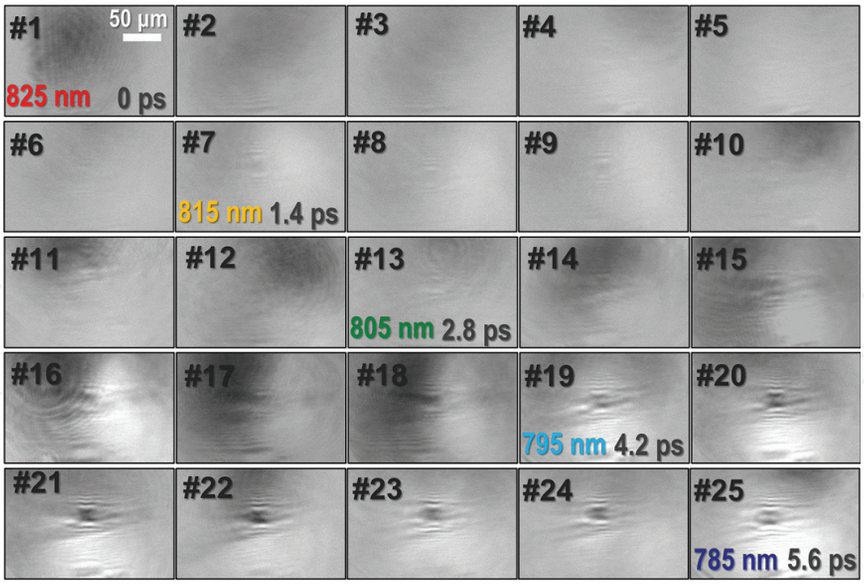

Figure 19. Motion picture of plasma filaments [20].

5. Conclusion

In this chapter, we introduced the motion picture camera called STAMP and presented motion pictures of femtosecond laser ablation. STAMP performs single-shot image acquisition without the need for repetitive measurements and without sacrificing high temporal resolution and image quality. The principle of this imaging method is based on the all-optical mapping of time-varying spatial profiles of target. We introduced two examples of the STAMP configurations: STAMP utilizing the spectral shaper and utilizing the spectral filtering and spectral broadening. The recording parameter such as the time window, the temporal resolution, and the number of frames can be tuned by changing the configuration of STAMP components, especially a temporal mapping device and a spatial mapping device.

By using STAMP, we obtained sequential images of sub-nanosecond dynamic events under the process of femtosecond laser ablation. Laser breakdown induced by intense femtosecond laser pulse was monitored with a frame interval of 15.3 ps and a total of six frames. The movie clearly shows the plasma generation and expansion on glass surface. Plasma filamentation generated inside a glass was also visualized with a frame interval of 230 fs and total of 25 frames. As demonstrated in this chapter, STAMP is a useful tool to understand precise processes of complex dynamics in ultrashort laser ablation.

Acknowledgements

The present work was supported in part by the Translational Systems Biology and Medicine Initiative from the Ministry of Education, Culture, Sports, Science and Technology (MEXT),

Japan, the Photon Frontier Network Program of MEXT, a Grant-in-Aid from the Japan Society for the Promotion of Science, and a Grant-in-Aid for the Program of Leading Graduate Schools of Keio University for "Science for Development of Super Mature Society" from MEXT.

Author details

Keiichi Nakagawa[1]*, Takakazu Suzuki[2] and Fumihiko Kannari[2]

*Address all correspondence to: kei@bmpe.t.u-tokyo.ac.jp

1 University of Tokyo, Japan

2 Keio University, Japan

References

[1] Momma C, Chichkov BN, Nolte S, Alvensleben F, Tunnermann A, Welling H, Wellegehausen B. Short-pulse laser ablation of solid targets. Optics Communication. 1996;**129**(1-2):134-142. DOI: 10.1016/0030-4018(96)00250-7

[2] Vogel A, Venugopalan V. Mechanisms of pulsed laser ablation of biological tissues. Chemical Reviews. 2003;**103**(2):577-644. DOI: 10.1021/cr010379n

[3] Ilday FÖ, Kerse C, Kalaycioglu H, Elahi P, Yavas S, Kesim D, Akçaalan Ö, Çetin B, Öktem B, Asik M, Hoogland H, Holzwarth R. Ablation-cooled material removal with ultrafast bursts of pulses. Nature. 2016;**537**:84-88. DOI: 10.1038/nature18619

[4] Toyoda K, Takahashi F, Takizawa S, Tokizane Y, Miyamoto K, Morita R, Omatsu T. Transfer of light helicity to nanostructures. Physical Review Letters. 2013;**110**(14):143603. DOI: 10.1103/PhysRevLett.110.143603

[5] Nakagawa K, Iwasaki A, Oishi Y, Horisaki R, Tsukamoto A, Nakamura A, Hirosawa K, Liao H, Ushida T, Goda K, Kannari F, Sakuma I. Sequentially timed all-optical mapping photography (STAMP). Nature Photonics. 2014;**8**:695-700. DOI: 10.1038/nphoton.2014.163

[6] Jussim E, Kayafas G, Edgerton H. Stopping Time: The Photographs of Harold Edgerton. New York, NY: Harry N. Abrams; 1987. p. 167

[7] Ray SF. High Speed Photography and Photonics. Bellingham, Washington, USA: SPIE Publications; 2002. p. 424

[8] Gattass RR, Mazur E. Femtosecond laser micromachining in transparent materials. Nature Photonics. 2008;**2**:219-225. DOI: 10.1038/nphoton.2008.47

[9] Tochigi Y, Hanzawa K, Kato Y, Kuroda R, Mutoh H, Hirose R, Tominaga H, Takubo K, Kondo Y, Sugawa S. A global-shutter CMOS image sensor with readout speed of 1-Tpixel/s

burst and 780-Mpixel/s continuous. IEEE Journal of Solid-State Circuits. 2013;**48**:329-338. DOI: 10.1109/JSSC.2012.2219685

[10] Gelderblom EC, Vos HJ, Mastik F, Faez T, Luan Y, Kokhuis TJ, van der Steen AF, Lohse D, de Jong N, Versluis M. Brandaris 128 ultra-high-speed imaging facility: 10 years of operation, updates, and enhanced features. The Review of Scientific Instruments 2012;**83**:103706. DOI: 10.1063/1.4758783

[11] Versluis M. High-speed imaging in fluids. Experiments in Fluids. 2013;**54**:1458. DOI: 10.1007/s00348-013-1458-x

[12] Feng J, Shin H, Nasiatka R, Wan W, Young A, Huang G, Byrd J, Padmore H. An X-ray streak camera with high spatio-temporal resolution. Applied Physics Letters. 2007;**91**:134102. DOI: 10.1063/1.2793191

[13] Tamamitsu M, Nakagawa K, Horisaki R, Iwasaki A, Oishi Y, Tsukamoto A, Kannari F, Sakuma I,Goda K. Design for sequentially timed all-optical mapping photography with optimum temporal performance. Optics Letters. 2015;**40**(4):633-636. DOI: 10.1364/OL.40.000633

[14] Weiner AM, Leaird DE, Patel JS, Wullert JR. Programmable shaping of femtosecond optical pulses by use of 128-element liquid crystal phase modulator. IEEE Journal of Quantum Electronics. 1992;**28**:908-920. DOI: 10.1109/3.135209

[15] Hashimoto K, Mizuno H, Nakagawa K, Horisaki R, Iwasaki A, Kannari F, Sakuma I, Goda K. High-speed multispectral videography with a periscope array in a spectral shaper. Optics Letters. 2014;**39**:6942-6945. DOI: 10.1364/OL.39.006942

[16] Hagen NA, Kudenov MW. Review of snapshot spectral imaging technologies. Optical Engineering. 2013;**52**:090901. DOI: 10.1117/1.OE.52.9.090901

[17] Mao X, Mao SS, Russo RE. Imaging femtosecond laser-induced electronic excitation. Applied Physics Letters 2003;**82**:697-699. DOI: http://dx.doi.org/10.1063/1.1541947

[18] Hu W, Shin YC, King G. Early-stage plasma dynamics with air ionization during ultrashort laser ablation of metal. Physics of Plasmas 2011;**18**:093302. DOI: http://dx.doi.org/10.1063/1.3633067

[19] Zhao X, Shin YC. Coulomb explosion and early plasma generation during femtosecond laser ablation of silicon at high laser fluence. Journal of Physics D: Applied Physics. 2013;**46**:335501. DOI: 10.1088/0022-3727/46/33/335501

[20] Suzuki T, Hida R, Ueda R, Isa F, Nakagawa K, Kannari F. Single-shot ultrafast 2D-burst imaging by STAMP utilizing spectral filtering (SF-STAMP). In: Santa Fe . New Mexico, USA: Santa Fe Community Convention; 2016. UTh4A.18

[21] Suzuki T, Isa F, Fujii L, Hirosawa K, Nakagawa K, Goda K, Sakuma I, Kannari F. Sequentially timed all-optical mapping photography (STAMP) utilizing spectral filtering. Optics Express. 2015;**23**:30512-30522. DOI: 10.1364/OE.23.030512

[22] Suzuki T, Hida R, Yamaguchi Y, Nakagawa K, Saiki T, Kannari F. Single-shot 25-frame burst imaging of ultrafast phase transition of $Ge_2Sb_2Te_5$ with a sub-picosecond resolution. Applied Physics Express. 2017;**10**:092502. DOI: 10.7567/APEX.10.092502

[23] Gabolde P, Trebino R. Single-frame measurement of the complete spatiotemporal intensity and phase of ultrashort laser pulses using wavelength-multiplexed digital holography. Journal of the Optical Society of America B. 2008;**25**(6):A25-A33. DOI: 10.1364/JOSAB.25.000A25

[24] Guang Z, Rhodes M, Davis M, Trebino R. Complete characterization of a spatiotemporally complex pulse by an improved single-frame pulse-measurement technique. Journal of the Optical Society of America B. 2014;**31**(11):2736-2743. DOI: 10.1364/JOSAB.31.002736

IntechOpen